



Green
Chemistry

**Strikingly High Amount of Tricin-lignin Observed from
Vanilla (*Vanilla planifolia*) Aerial Roots**

Journal:	<i>Green Chemistry</i>
Manuscript ID	GC-ART-10-2021-003625.R1
Article Type:	Paper
Date Submitted by the Author:	23-Nov-2021
Complete List of Authors:	Li, Mi; University of Tennessee, Chemical and Biomolecular Engineering Pu, Yunqiao; Oak Ridge National Laboratory, Joint Institute of Biological Science, Biosciences Division Meng, Xianzhi; University of Tennessee, Chen, Fang; University of North Texas, Materials and Mechanical and Energy Engineering Dixon, Richard; University of North Texas, Materials and Mechanical and Energy Engineering Ragauskas, Arthur; University of Tennessee Knoxville College of Engineering,

SCHOLARONE™
Manuscripts



Strikingly High Amount of Tricin-lignin Observed from Vanilla (*Vanilla planifolia*) Aerial Roots

Mi Li^a, Yunqiao Pu^{* b,c,d}, Xianzhi Meng^e, Fang Chen^f, Richard A. Dixon^f, Arthur J. Ragauskas^{* a,b,c,d,e}

Received 00th January 20xx,
Accepted 00th January 20xx

DOI: 10.1039/x0xx00000x

Notice: This manuscript has been authored by UT-Battelle, LLC under Contract No. DE-AC05-00OR22725 with the U.S. Department of Energy. The United States Government retains and the publisher, by accepting the article for publication, acknowledges that the United States Government retains a non-exclusive, paid-up, irrevocable, world-wide license to publish or reproduce the published form of this manuscript, or allow others to do so, for United States Government purposes. The Department of Energy will provide public access to these results of federally sponsored research in accordance with the DOE Public Access Plan (<http://energy.gov/downloads/doe-public-access-plan>).

Lignin has attracted tremendous interest as a renewable source for biofuels, biomaterials, and chemicals especially in the era of bio-based refineries. Arising primarily from phenylpropanoid, lignin is biosynthesized and occurs abundantly in most terrestrial plants with complex structures. The structural studies of lignin play an essential role in both understanding the nature and biosynthesis of these polymers and optimizing their valorization values. In this study, we have investigated the structures of lignin from different tissues—aerial roots, nodes, internodes, and seeds, from vanilla (*Vanilla planifolia*) by gel permeation chromatography (GPC), heteronuclear single-quantum coherence (HSQC) nuclear magnetic resonance (NMR), and ³¹P NMR. An unusual triclin-lignin was observed in the aerial roots of vanilla with an extremely high level of triclin unit (194%) and *p*CA (71%) over the sum of syringyl and guaiacyl (S+G) units, whereas the lignin from the nodes and internodes displayed traditional S/G type lignin with only 4–10% triclin abundance. Consistent with other reports of C-lignin, the seeds lignin is primarily composed of caffeyl alcohol. The aerial roots lignin is primarily consisted of β-O-4' alkyl-aryl ether substructures (96% of linkages) in comparison to 65 and 73% in the nodes and internodes lignin, respectively. Thioacidolysis quantification results showed that that lignin from aerial roots has 29.1 mg/g triclin, about 3- to 5-fold higher than in lignins isolated from nodes (10.1 mg/g) and internodes (6.9 mg/g). This communication of a particularly high level of triclin-lignin in Vanilla has important impacts in two-folds: (1) the presence of the high amount of triclin as part of lignin from aerial roots could play a vital role for the valorization of lignin, even triclin itself, as a feedstock for value-added chemicals and commodities; and (2) it could open new ways to scientists to design and engineer the structure of triclin-lignin, or lignin in general, to confer plants with new or improved properties due to the plasticity of lignification.

Introduction

The growing interest in bioeconomy warrants a consensus that lignin valorization is an essential strategy for environmental sustainability and economics of the lignocellulosic biorefinery operations.^{1, 2} Lignin is a complex aromatic heteropolymer derived primarily from three canonical monolignols *p*-hydroxycinnamyl alcohols (i.e., *p*-coumaryl, coniferyl, and sinapyl alcohols), differing in their degrees of methoxylation

and forming *p*-hydroxyphenyl (H), guaiacyl (G), and syringyl (S) units in lignin, respectively.³ The oxidation or dehydrogenation of monolignols followed by radical coupling reactions gives rise to a complex phenylpropanoid polymer characterized with variously interconnected monomer-derived units through ether and carbon-carbon linkages.⁴ Ultimately, lignin deposits in plant cell walls providing physical and mechanical support, enable long-distance water and solute transportation, and is a barrier to herbivores and pathogens.⁵ Lignin has been deemed as one of the most recalcitrant factors in the plant cell wall hindering effective utilization and conversion of lignocellulosic biomass.⁶ Although lignin has been studied with remarkable progression, its compositional and structural details are still not fully understood or defined due to its complexity and heterogeneity.

Recent discoveries of lignin monomers beyond the canonical monolignols challenge and expand the traditional definition of lignin and lignification in the cell wall. These non-conventional lignin structural units have been grouped into (1) phenylpropanoid-pathway-derived monomers, including

^a Center for Renewable Carbon, Department of Forestry, Wildlife and Fisheries, University of Tennessee (UT), Knoxville, TN.

^b Center for Bioenergy Innovation.

^c Biosciences Division, Oak Ridge National Laboratory (ORNL), Oak Ridge, TN.

^d UT-ORNL Joint Institute for Biological Sciences, Oak Ridge, TN

^e Department of Chemical and Biomolecular Engineering, UT, Knoxville, TN.

^f BioDiscovery Institute and Department of Biological Sciences, University of North Texas, Denton, TX.

Electronic Supplementary Information (ESI) available: [details of any supplementary information available should be included here]. See DOI: 10.1039/x0xx00000x

monolignol ester conjugates (i.e., conjugates with acetates, p-coumarates, p-hydroxybenzoates, ferulate, and benzoates analogs), monolignols precursors (i.e., hydroxycinnamaldehydes) and intermediates (i.e., caffeyl and 5-hydroxyconiferyl alcohols), and others (i.e., dihydroconiferyl alcohol, guaiacylpropane-1,3-diol, and hydroxycinnamate esters/cross-linking etc.);^{4, 7} and (2) non-phenylpropanoid-pathway-derived monomers, including flavonoids (i.e., tricrin, selgin, naringenin, and apigenin), hydroxystilbene (i.e., piceatannol, resveratrol, isorhapontigenin, and their *O*-glucosides), hydroxycinnamamides (feruloyltyramine, diferuloylputrescine).^{4, 8, 9} The hypothesis of combinatorial coupling of these non-canonical monomers with monolignols have been corroborated and analyzed by both experimental and computational methods.^{4, 10} These results continuously reveal new structural features indicating that plants are capable of using a wide variety of phenolic compounds for lignification.

The incorporation of tricrin, one type of flavonoid, to lignin polymer has been shown to be of particular interest and been extensively studied. Tricrin typically occurs in plants in extractable form, such as free tricrin, tricrin-glycosides, flavonolignan glycosides, or low-molecular-weight flavonolignans (or flavonolignols).¹¹ Due to its promoting effects on human health, tricrin has been extensively studied for its biological, nutraceutical, and pharmaceutical importance.¹² As one type of flavone, tricrin is typically originated from a combination of shikimate-derived phenylpropanoid and the acetate/malonate-derived polyketide biosynthetic pathways that is out of the canonical monolignols biosynthesis.¹¹ However, tricrin-lignins, defined as lignins containing tricrin structural unit, have been recently discovered with a wide distribution primarily in monocotyledonous plants (both grass and nongrass) and certain eudicotyledonous species.^{11, 13} Reported plants that have tricrin-lignins include Alfalfa¹³, Arundo¹⁴, bamboo¹⁵, barley¹⁶, carex¹⁷, coconut coir¹⁸, giant reed¹⁹, maize²⁰⁻²², rice²³⁻²⁷, wheat^{23, 28-30}, sugarcane³¹, and wood³². The discovery of tricrin-lignins indicates a tight relationship between the two major downstream metabolites, monolignols, and flavonoids, in the phenylpropanoid biosynthetic pathway in grasses.

Manipulation of transcriptional regulatory network involved in secondary cell wall formation has shed informative highlight on the biosynthetic mechanism of tricrin incorporation with lignification. For example, overexpression of *AtMYB61*²⁷, suppression of *OsMYB108*³³ and *C3'H*²⁶ of the rice plant, resulted in increased tricrin moieties in lignin. In maize, silencing *C2-Idf* resulted in reduced tricrin-lignin,³⁴ whereas suppression of *CAD2* leads to increased tricrin level in maize lignin.³⁵ While tricrin is marginally reduced in *COMT* suppressed barley³⁶, sorghum³⁷, maize³⁸, Lam et al. found that *COMT* has a bifunctional role in the biosynthesis of tricrin and monolignols (i.e., S units), leading to tricrin-lignin formation in rice.³⁹ They also found that *FLAVONE SYNTHASE II* (*OsFNSII*)⁸ and flavonoid 3'-hydroxylases (*OsA3'H/C5'H*)⁹ are responsible for the formation of tricrin-lignins or its analogs in the rice cell wall. In the flavonoid 3'-hydroxylases enzymes, specifically, *CYP75B3* primarily works with *OsF2H* for the biosynthesis of flavone C-

glycosides, whereas *CYP75B4* functions together with *OsFNSII* in the biosynthesis of ricin-bound lignin.⁹ However, *CCoAOMT* suppression appears not to be essential for tricrin-lignin biosynthesis in maize³⁸. Moreover, tricrin is contended to be a nucleating site for lignification, and aryl ether (4'-*O*-β) has only been identified and suggested for the linkage between tricrin and lignin monolignols.^{21, 40} However, a full understanding of how the biosynthetic pathway of monolignols and flavonoids merge in the plant lignification has not been determined.

The distributions of tricrin in the plant kingdom vary in the species and even the tissue of the family, typically in the level of milligram per gram tissue.¹¹ The content of lignin-integrated tricrin turns to be several folds higher than the extractable tricrin and tricrin-lignan levels, for instance, in wheat, maize, oat, and rice.¹³ Another study showed that a high concentration of tricrin derivatives (30-35%) was detected in the lyophilized liquid fractions of ultrasound and hydrodynamic cavitation pretreated wheat straw.⁴¹ Given the fact that a large quantity of lignin (over 62 million tons) is generated annually from pulp and paper industry, and biorefining processes¹, and the potential values of tricrin to human health as antioxidant, anti-aging, anticancer, and cardioprotective agents, seeking alternative plant source with a high level of tricrin-lignin becomes essential in making the valorization of tricrin-lignin economically feasible.

In this study, we analyzed lignin structure and compositions from four tissues of vanilla (*Vanilla planifolia*)—aerial roots, nodes, internodes, and seeds coat (Fig. 1). Specifically, we report for the first time here that the lignin isolated from aerial roots had an extremely higher level of tricrin units in tricrin-lignin, in contrast to the lignins isolated from vanilla nodes and internodes. The exceptional proportion of tricrin in tricrin-lignin provides important insights to further understand the plasticity of the lignification process, lignin structure in plants, and enhance lignin valorization in terms of tricrin-derivatives.

Results and discussion

Significantly higher cellulolytic enzyme lignin (CEL) yield from aerial roots of vanilla.

Since the yield of cellulolytic enzyme lignin (CEL) is affected by the ball milling conditions,⁴² it was anticipated that progressive mechanical treatment facilitated the disruption of plant cell wall allowing for more lignin released from associated carbohydrates hence more extracted lignin and higher CEL.⁴³

Fig. 1. Vanilla tissues (aerial roots, nodes, internodes, and seeds) used for cellulolytic enzyme lignin (CEL) isolation and lignin structural characterization.



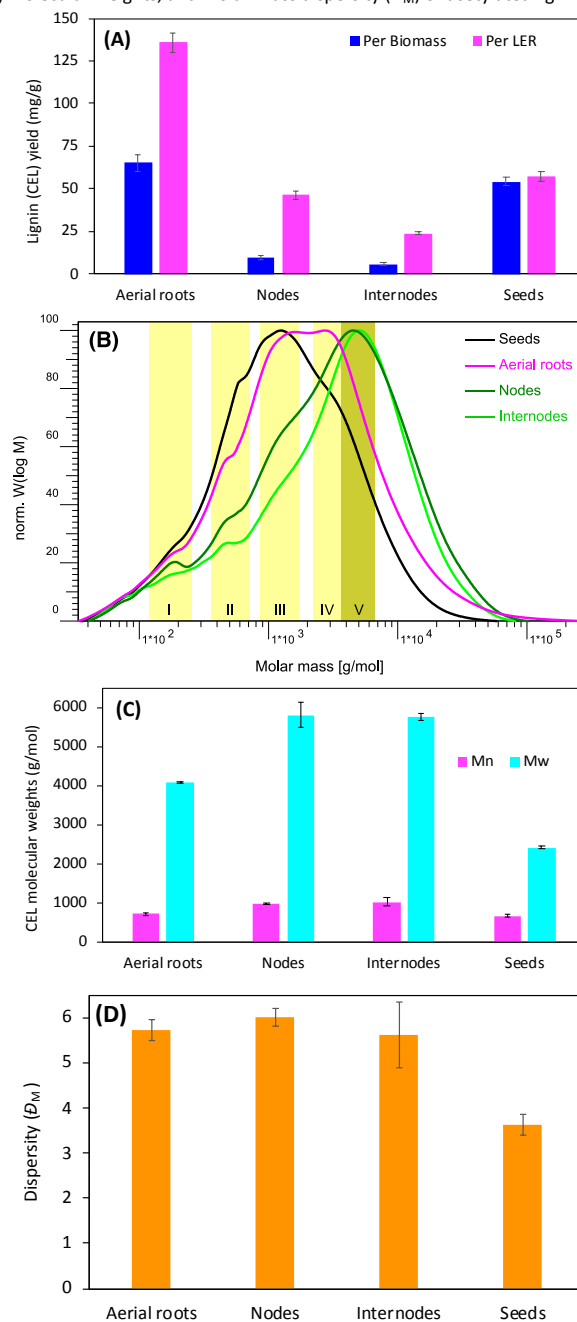
To minimize the effect resulting from different milling conditions, tissues were cut into similar size (<0.43 mm) with a Wiley mill, loaded with the same amount, and ball milled with the same protocol (number of balls charged, amount of time, rotation speed, and rest intervals). We found that CEL yield varied significantly on the tissues used for lignin isolation, and was in the order of aerial roots, seeds, nodes, and internodes from high to low based on dry biomass weight (Fig. 2A). The weight loss, calculated from the remaining weight of lignin enriched residue (LER) and resulted primarily from carbohydrates removal during enzymatic hydrolysis, was remarkably dependent on the tissues too. Agreeing with a study by Chen et al.,⁴⁴ nodes and internodes had a similar weight loss of 76–78% whereas aerial roots only had 52%, which indicates that the aerial roots have about twice as much LER as the nodes and internodes. On contrary, only 5% weight loss was observed on vanilla seeds, which is attributed to the larger amount of lignin contained in the seed coats.⁴⁴ The nodes had about twice the CEL yield compared with the internodes, which is likely related to the lignin distribution. For example, wheat straw node generally has higher lignin content than internode.⁴⁵ The aerial roots had dramatically higher CEL yields (5 times and 2 times higher based biomass and LER mass, respectively) than the nodes. These results suggest that the aerial roots, with extremely higher CEL yields, are a special vanilla tissue from other tissues such as nodes, internodes, and seeds.

Molecular weights distribution of acetylated lignin.

The molecular weight of lignin is a fundamental property impacting the recalcitrance of biomass and the valorization of lignin. To assure its solubility in tetrahydrofuran, CELs were acetylated before the measurement of the molecular weight using gel permeation chromatography (GPC). The molecular-weight profiles of acetylated lignin displayed broad chromatograms distributions spanning a range from a couple of hundreds up to 10^5 g/mol (Fig. 2B). The molecular weight distribution profiles could be divided mainly into five zones indicated by the yellowish bands corresponding to molecular weights close to 200, 500, 1,000, 3,000, and 5,000 g/mol, respectively. The major lignin molecular size peaked at 1,000 g/mol for seeds, 1,000–4,000 g/mol for aerial roots, and 4,000–6,000 g/mol for nodes and internodes. The wide-spanning range of GPC profiles indicates a broad lignin molecular weight distribution. Based on the GPC elution profile, the CELs contained small proportions of lignin compounds with molecular weights lower than 1,000 g/mol, which indicating the presence of lignin oligomers. The average molecular weight calculated against the calibration curve prepared using a series of standard polystyrene showed that the nodes and internodes lignins had similar molecular weights with weight-average molecular weight (M_w) of 5,600–5,700 g/mol and M_n of 950–1,025 g/mol whereas the lignin from aerial roots had strikingly (30–40%) lower M_w of 4,091 g/mol and M_n of 715 g/mol (Fig. 2C). However, the lignins from these three tissues displayed comparable molar-mass dispersity (D_M) 6.0 (Fig. 2D) suggesting

a similar heterogeneity of isolated CELs. In line with an earlier report, the seed lignin, primarily comprised of caffeyl alcohol (C-lignin, see more below), only accounts for one-third of M_w of stem lignin.⁴⁴ Based on these findings, the aerial roots lignin exhibited a very different molecular mass compared with stems (nodes and internodes) lignins. The lower molecular weights of the aerial roots lignin are likely associated with the higher tricin compositional units in the lignin (see more discussion below).

Fig. 2. Yield and molecular size of lignins from different tissues of vanilla. CEL: cellulytic enzyme lignin; number-average (M_n), weight-average (M_w) molecular weights, and molar-mass dispersity (D_M) of acetylated lignins.



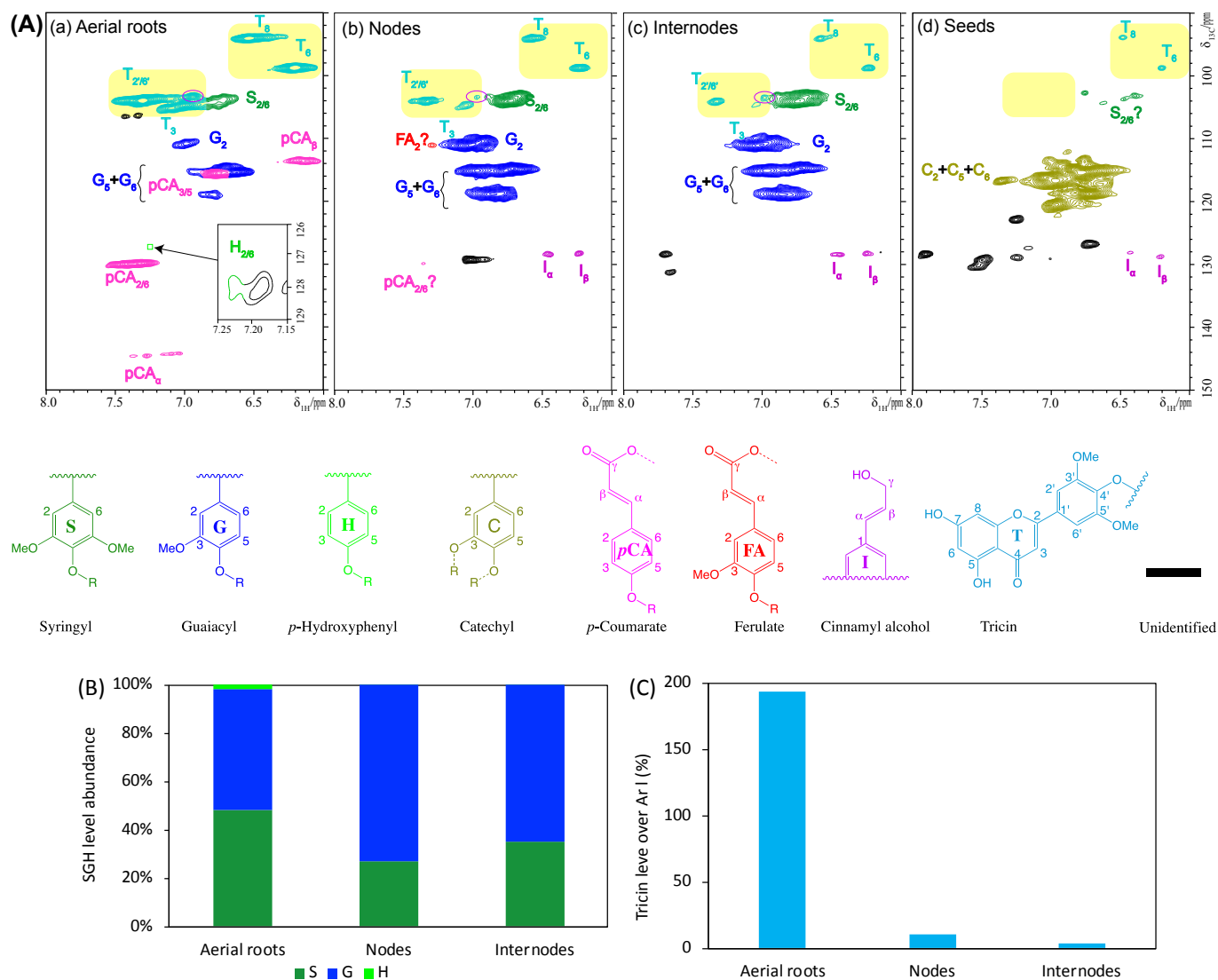


Fig. 3. Short-range (aromatic regions only) ^{13}C - ^1H correlation HSQC spectra and semi-quantification of lignin subunits. (A) HSQC spectra of CELs from *V. planifolia* aerial roots (A), nodes (B), internodes (C), and seed coat (D) in $\text{DMSO}-d_6$. Contours corresponding to color-coded structures in this region are used to measure the relative abundance of S, G, H, and T over S+G+H. δ , chemical shift; ppm, parts per million. Relative abundance of S, G, H units (B) and triclin (C) over aromatic regions (S+G+H).

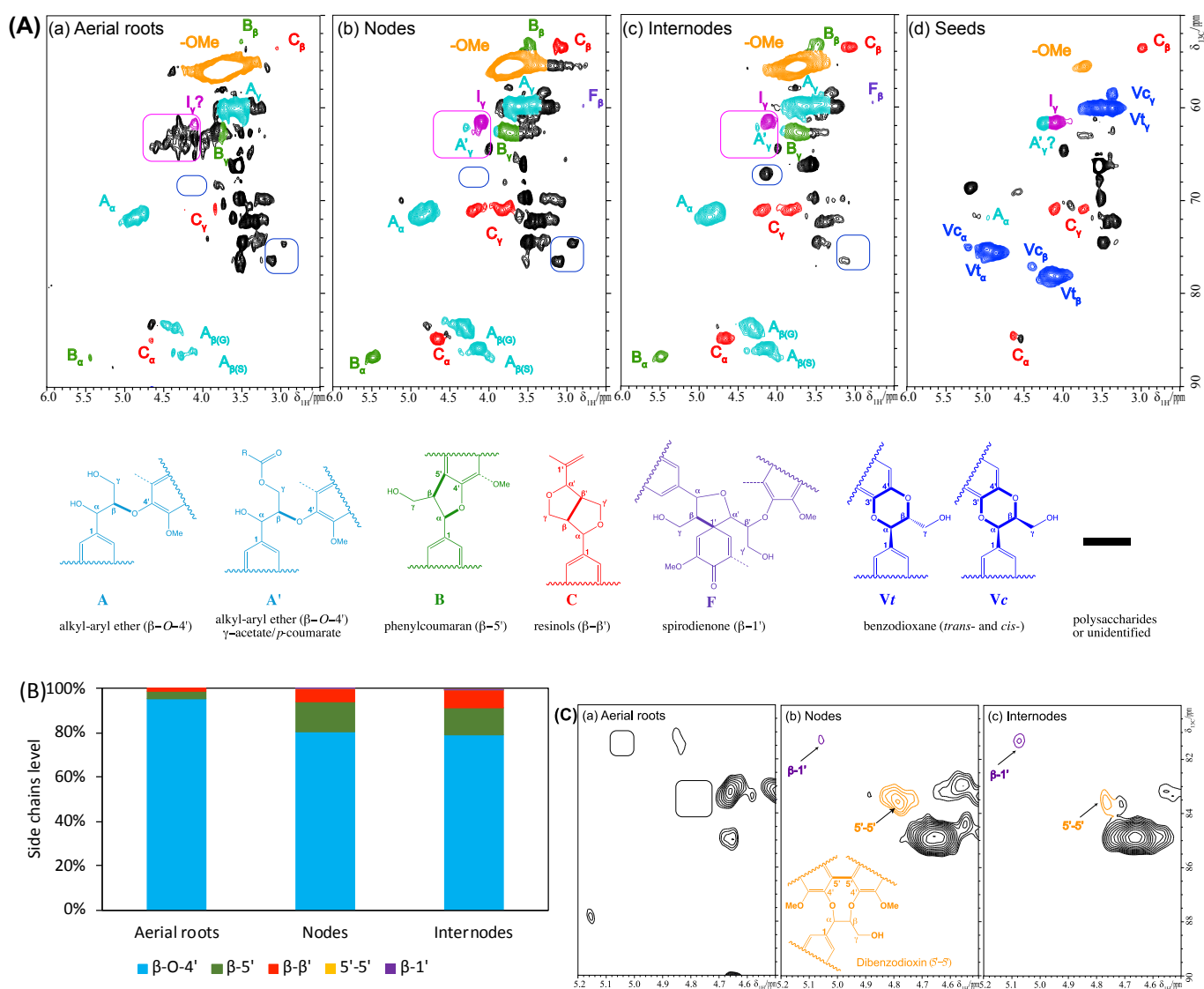


Fig. 4. Short-range ^{13}C - ^1H correlation (HSQC) spectra of isolated lignins from aerial roots, nodes, internodes, and seed of *V. planifolia* and quantification of lignin side-chain linkages. (A) NMR spectra of CELs (aliphatic regions only) in $\text{DMSO}-d_6$. (B) Relative abundance of inter-units linkage over total linkages. (C) 5'-5' & β -1' linkages observed in nodes and internodes lignins. Contours corresponding to color-coded structures in this region are used to measure the relative level of interunit linkages.

2D HSQC NMR revealing special compositional triclin lignin in aerial roots.

Two-dimensional (2D) NMR is a powerful and widely used technique in elucidating lignin structural features including compositional units and interunit linkages.⁴⁶ The lignins isolated from the separated tissues were dissolved in $\text{DMSO}-d_6$ and characterized by 2D HSQC NMR using the chemical shifts of those related cross-signals are listed in Table S1. The spectra depicting the aromatic region of CELs exhibited predominant lignin signals (Fig. 3A). Specifically, the aerial roots, nodes, and internodes spectra displaying typical S/G type lignin and the seeds exhibited a C-lignin structure, a homopolymer comprised of caffeyl alcohol, are in agreement with those vanilla lignins reported previously.⁴⁴ We also detected a small level of cross-peaks tentatively attributed S units. However, it is worth mentioning that the seeds of several dicot plants have been

reported to produce C-lignin together with G/S lignins.⁴⁷ The S/G ratio of nodes lignin (0.37) is slightly lower than that of internodes lignin (0.55) whereas the aerial roots lignin contains a similar abundance of S to G unit (S/G ratio equals 0.96) as well as a small amount of H unit (Fig. 3B).

We also found a substantial amount of triclin (T) units in the nodes and internodes lignins (yellowish block area in Fig. 3A), which is consistent with the results reported by Lan et al. showing that triclin occurred in a moderate amount of stem and leaf of three *Vanilla* species (i.e., *Vanilla planifolia*, *Vanilla planifolia*, and *Vanilla phalaenopsis* with 12–15 mg/g lignin).¹³ A small amount of triclin contour together with a small amount of S unit were observed in seed lignin mentioned above. The coexistence of C-lignin and S/G lignin have been reported in several dicot plants (*Euphorbiaceae* and *Cleomaceae*) that produce C-lignin together with traditional G/S lignins in their seed coats.^{47, 48} Surprisingly, the aerial roots lignin

demonstrated a tremendous signal intensity of triclin beside G and S units. The relative amount of triclin over the aromatic region, on a basis of contour size of T_6 was around 194% in aerial roots lignin in comparison to 10% and 4% in nodes and internodes lignin, respectively (Fig. 3C). Clearly, the considerably intense signal in 2D HSQC NMR spectra revealed that CEL from the aerial roots had a substantial amount of triclin compared with those from nodes and internodes, although it should be noted that terminal end units (i.e., triclin here) are nonlinearly and might be overestimated in the HSQC spectra due to much slower relaxation.⁴⁹ Thus, the volume integrals of triclin end unit likely overrepresent their quantitation amount, however, comparative study of the triclin over aromatics ratio between aerial root and stem is undoubtedly remarkable. Based on the results of 10.50 mg/g lignin reported on *Vanilla planifolia* stem,¹³ we contended that the aerial roots of *Vanilla planifolia* in our study could have a level of ~200 mg/g lignin by the semi-quantitative comparison of contour volume-integration. Additionally, the strikingly high amount of triclin could be partially derived from free triclin as shown by the contour in the oval-shaped line (Fig. 3A), and triclin-lignans as shown in the bands of small molecular weights (<1,000 g/mol, Fig. 2B), due to their slightly different chemical shifts in the HSQC spectra. Taken together, the aerial roots of *Vanilla planifolia* presented a considerably higher amount of triclin units than the stem (nodes and internodes).

Additionally, we also detected a substantial amount of pCA (71% over aromatic, Fig. S1) and a small amount of H unit (1.6%) in aerial roots CEL (Fig. 3B) whereas the nodes and internodes lignin had non-detectable contours of pCA and only a trace amount of H unit (<0.1%). The aerial roots lignin had a slightly higher FA content (3.6%) compared with those from nodes and internodes (1-2%). Another structural difference observed between the CELs from the three tissues was the amount of cinnamyl alcohol end unit (I), with 2-3% in nodes and internodes versus non-detectable signal in aerial roots (Fig. S1). The aromatic units in seeds lignin were dominated with C units with a small amount of cinnamyl alcohol end units according to previous research identification.⁴⁴ Taken together, the NMR spectra results revealed that the CEL from aerial roots has a considerably different lignin compositional structure in terms of triclin, pCA, and FA level from those from nodes and internodes.

2D HSQC NMR revealing interunit linkages of lignins.

Lignin structure is mainly depicted by its prominent interunit linkages. The aliphatic side-chain region of these CELs was compared to further understand their characteristic interunit bonding patterns (Fig. 4) and the chemical shifts of these identified linkages were listed in Table S1. For the S/G type lignins, CELs from aerial roots, nodes, and internodes, HSQC NMR spectra revealed that the lignin interunit linkages are primarily composed of β -O-4' ethers (>80%, Fig. 4B). The abundance of these typically predominant linkages is comparable with these reports for other non-woody biomass such as switchgrass⁵⁰ and sugarcane straw.³¹ Particularly, the aerial roots lignin had significantly higher 96% β -O-4' ethers and less amount of β -5' and β - β' (1-3%) in comparison to the nodes

and internodes lignin (Fig. 4B). However, no 5-5' and β -1' linkages were detected in aerial roots whereas a trace amount of these linkages (<1%) existed in nodes and internodes lignin (Fig. 4C). For the seeds lignin, the most prevalent linkages are benzodioxane type, a result from caffeoyl alcohol coupling, supplemented with minor amount of β - β' , which is consistent with previous identification.⁴⁴ Additionally, we tentatively identified a trace amount of β -O-4' ethers that is in line with the small amount of S unit and triclin contours in the aromatic/unsaturated region of the HSQC spectra (Fig. 3A). Other noticeable differences lied in the aliphatic region of HSQC NMR spectra between the aerial roots and stem (nodes and internodes) are marked by pink and blue round rectangles which may be attributed to the presence of carbohydrates (Fig. 4A). The overall HSQC NMR spectra of the side chain region only provide the semi-quantitated abundance of three prevalent linkages with limited information of significantly distinguished bonding between the aerial roots and nodes/internodes to our current knowledge. The importance of these unidentified cross-peaks in aerial roots lignin needs further investigation (pink blocks in Fig. 4A).

It has been proposed that triclin can only link with lignin macromolecule via 4'-O-coupling with a monomer, meaning that each lignin molecule can contain at most one triclin structural unit and triclin has been contended as a nucleation site in lignification.²¹ When more triclin is present in the aerial root cells, a higher chance of lignification will be involved in the cross-coupling of triclin with a monolignol than of monomer-monomer coupling. More lignin macromolecules are therefore anticipated with the presence of a relatively higher concentration of triclin. Although there are likely a diverse of factors influencing degree of polymerization in the plant cell wall, it is, therefore, reasonable to expect a relatively higher triclin level is associated with a lower molecular weight of lignin in the tissue. This correlation explains the reason, at least partially, for the much lower lignin molecular size in aerial roots lignin (higher triclin level, M_w ~4,000 g/mol) than stem lignin (lower triclin level, M_w ~6,000 g/mol) observed above (Fig. 2C).

Lignin functional groups elucidated by ³¹P NMR.

³¹P NMR spectroscopy has been widely applied for differentiating and quantitating the different types of hydroxyl groups (OHs) including aliphatic, carboxylic, guaiacyl, syringyl, C₅ substituted phenolic hydroxyls, and *p*-hydroxyphenyls in lignin⁵¹. We recently have used ³¹P NMR to qualify flavonoids and specifically to identify the presence of triclin units in corn stover lignin.⁵² Considering the exclusive C-type lignin in seeds, only these various OHs of CELs from aerial roots, nodes, and internodes were determined using ³¹P NMR (Fig. 5). In accordance with the results revealed in HSQC, aerial roots exhibited a strikingly higher (~3 times higher than nodes and internodes) on the OHs derived from triclin units (Fig. 5B). The significantly lower OH on 4' position of triclin than 5 and 7 positions suggests a great deal of triclin units has been linked to lignin macromolecules at 4'OH in the form of 4'-O- β ether bond.^{21, 53} The presence of 4'OH (0.09 mmol/g lignin) revealed in ³¹P

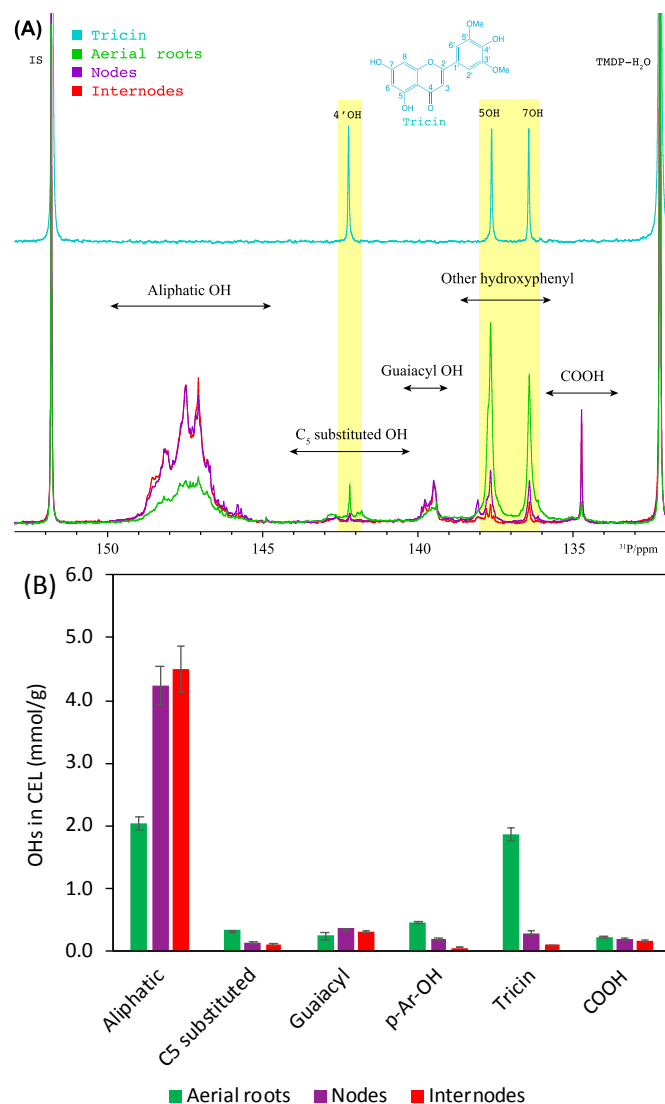


Fig. 5. Lignin functional groups determined using ^{31}P NMR. A: ^{31}P NMR of triclin and CELs after phosphorylation. B: quantitative results of lignin hydroxyl groups (mmol/g lignin).

NMR spectra could be related to two reasons: (a) the presence of free form triclin as shown by the cross-peaks of free triclin units detected in HSQC (Fig. 2A); and (b) the presence of structurally similar flavonoids, for instance, syringetin has almost identical 4'OH chemical shift as that in triclin.⁵² The aerial roots lignin also showed considerably less amount of aliphatic OHs and a higher amount of p -hydroxyphenyls ($p\text{-Ar-OH}$) (Fig. 5B). Due to the potentially remained carbohydrates in the CELs (carbohydrates signals in Fig. 4), the aliphatic OHs could be partially contributed by non-lignin carbohydrates.⁵⁴ In harmony with this ^{31}P quantitative result, the anomeric region of HSQC spectra of aerial roots had no detectable polysaccharides than the nodes and internodes (Fig. S2). The higher $p\text{-Ar-OH}$ in aerial roots lignin is likely due to the higher amount of $p\text{CA}$ which is consistent with the HSQC spectra displaying a substantial amount of $p\text{CA}$. The amount of OHs derived from C_5 substituted, guaiacyl, and carboxylic structure in aerial roots lignin are comparable to those from nodes and internodes lignin.

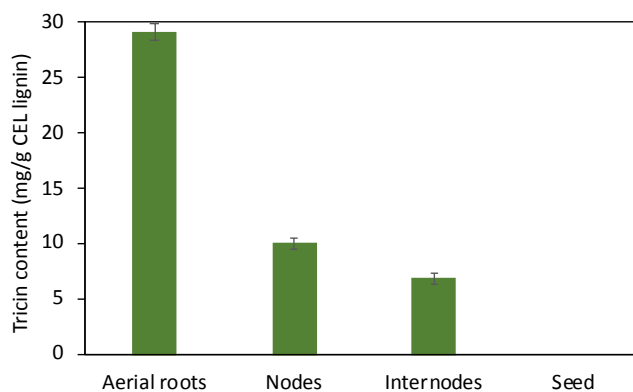


Fig. 6. Tricin content in isolated lignins from aerial roots, nodes, internodes, and seed of *V. planifolia* quantified by thioacidolysis. The error bar shows the standard deviation of biological duplicate samples.

Depolymerization of triclin-lignin and triclin quantification.

Although triclin and its derivatives with chemo-preventive activities have been employed extensively in the pharmaceutical^{11,55} and, to a lesser extent, dietary supplement sectors⁵⁶, not much has been examined on manipulating triclin-lignin for biorefinery applications. From the polysaccharide-oriented biorefinery perspective, the association of triclin-lignin with biomass recalcitrance based on the proposed role of triclin as a nucleation site for lignification has been investigated.^{21,40} Expression of plant triclin-related enzymes was manipulated to (1) alter lignin levels in cell walls and biomass digestibility and/or (2) modify lignin molecular size and depolymerization; however, the fundamental correlations remain elusive.⁵⁶ For example, the rice mutant completely devoid of triclin had enhanced enzymatic saccharification efficiency.⁸ Silencing the chalcone synthase gene revealed an overall positive correlation between the abundance of triclin and saccharification efficiency in the leaves of maize.³⁴ Another study of rice mutants also revealed this correlation, which was explained in terms of the increased level of triclin resulting in more nucleation sites for lignification, smaller lignin molecular weight and higher degradability of cell walls.³⁸ However, suppression of *CYB75B4* in rice led to cell walls with depleted triclin-lignin and enhanced saccharification yield.⁹ These data suggest that the fundamental relationships between triclin biosynthesis, lignin content and composition, and biomass recalcitrance remain unclear. Other studies reported that triclin was preferentially targeted and removed from lignin by certain white-rot fungi⁵⁷ and termites⁵⁸, which suggests that triclin may also play a crucial role in the microbial degradation of lignin. However, catalytic and bio-catalytic lignin depolymerization strategies for triclin-lignin are only now emerging as an intriguing subject despite the fact that numerous studies have focused on the conversions of the major monolignol-derived phenylpropane units in canonical lignin.⁵⁶

The thioacidolysis method has been widely used for lignin structure and compositional analysis.⁵⁹⁻⁶¹ It estimates the amount and composition of uncondensed aryl ether structures in lignin by cleaving lignin monomers that are only involved in

aryl ether linkages. Thioacidolysis also proved to be an efficient method in liberating triclin from triclin-lignin with little degradation for triclin quantification.^{13, 62} Therefore, we conducted thioacidolysis of the isolated lignin to, on the one hand, quantify the absolute triclin level in the studied tissues, and, on the other hand, to assess the feasibility of depolymerizing triclin-lignin to value-added triclin units. Consistent with our results of the triclin level revealed from HSQC spectra, thioacidolysis results showed that lignin from aerial roots has 29.1 mg/g triclin, about 3- to 5-fold higher than in lignins isolated from nodes (10.1 mg/g) and internodes (6.9 mg/g) (Fig. 6). No triclin is detected from seed lignin that almost exclusively consists of C-units as shown in HSQC spectra. The triclin levels of nodes and internodes agree well with those reported by Lan et al. in *Vanilla* species (i.e., 10.5 mg/g and 12.7 mg/g triclin in stem and leaf lignin, respectively).¹³ The quantitative results corroborate the exceptionally high level of triclin in the aerial roots of *Vanilla*. Comparable triclin amounts from other plants have been reported, such as 33.1 mg/g in oat, 32.7 mg/g in wheat, and 28.0 mg/g in *Brachypodium* based on lignin.¹³ The content of triclin in wheat straw leaves is higher than that in stem (17% vs 12% based on total HGS monolignols)⁶³, and the same is true in maize.³⁴ The relatively high triclin level in the aerial parts of plants is intriguing although its functional significance is unclear.

Conclusions

We have studied the structures of lignin isolated from different tissues of vanilla, aerial roots, nodes, internodes, and seeds. The nodes and internodes lignin show a typical S/G (a ratio of 0.4-0.5) type lignin whereas the seeds lignin is almost exclusively made of C units. A substantial amount of triclin (4-10% over S+G) has been found in the presence of nodes and internodes lignin. Particularly, the lignin from aerial roots displays a considerably higher amount of triclin with 194% over S and G based on the semi-quantification of NMR contours, which suggests a remarkably different triclin-lignin structure. Thioacidolysis results showed that lignin from aerial roots has 29.1 mg/g triclin, in comparison to 10.1 mg/g nodes lignin and 6.9 mg/g internodes lignin. The compositional differences are also reflected in differences in the relative abundances of the various interunit linkages revealed by 2D NMR. The lignin from aerial roots has more than 95% alkyl-aryl ether β -O-4' substructures whereas the nodes and internodes have 73% and 65%, respectively. These findings point out that a special triclin-lignin with strikingly high triclin unit has been isolated from aerial roots lignin. This high amount of triclin units relative to lignin traditional monolignols is valuable in maximizing the values of lignin to bio-products. The higher amount of triclin units in vanilla aerial roots could also extend its pharmaceutical application due to its health-promoting benefits. Lastly, the identification and depiction of aerial roots lignin provide important information for the diversity of lignin structure and better understanding lignin biosynthesis in plants. Upcoming research on the cleavage and quantification of triclin unit, and

the structural delineation of triclin-lignin from the aerial roots of *Vanilla* will be investigated in details.

Experimental

Cellulolytic enzyme lignin Isolation

The vanilla whole green plant (*Vanilla planifolia*) was provided by collaborators at the University of North Texas. The tissues of vanilla, including aerial roots and stems (nodes and internodes), were separated and manually cut into 1-2 cm pieces (Fig. S3). The vanilla seeds were provided separately after harvesting. The air dried biomass was thoroughly extracted with a mixture of toluene-ethanol (2/1 by v/v) in Soxhlet for 24 h and followed by acetone extraction for another 12 h. Cellulolytic enzyme lignin (CEL) was isolated from vanilla nodes, internodes, aerial roots, and seeds according to published literature procedure (Fig. S3).^{50, 64} In brief, the extractives-free samples were milled with a Wiley mill (Thomas Scientific, Model 3383-L10, Swedesboro, NJ) through a 40-mesh (0.425 mm) screen. About 1 g of the down-sized samples was loaded to 50 mL ZrO₂ grinding jar (including 10×10 ball bearings) in Retsch Ball Mill PM 100. The biomass was then ball milled at 580 RPM in a frequency of 5 min with 5 min pauses in-between for 1.5 h total time. The milled fine cell wall powder was then subjected to enzymatic hydrolysis with a mixture of Cellic[®] CTec2 and HTec2 (gift from Novozymes North America) in acetic acid/sodium acetate buffer (pH 4.8, 50°C) under continuous agitation at 200 rpm for 48 h. The residue was isolated by centrifugation and was hydrolyzed once more with freshly added enzymes mixture. The residue obtained was washed with deionized water (18.0 M Ω), centrifuged, and freeze dried, namely lignin-enriched residue. The lignin-enriched residue was extracted with dioxane-water (96% v/v, 10.0 mL/g biomass) for 24 h. The extracted mixture was centrifuged and the supernatant was collected. Dioxane extraction was repeated once by adding freshly distilled dioxane in water. The extracts were combined, roto-evaporated to reduce the volume at less than 45°C, and freeze dried. The obtained lignin samples, designated as CEL, was used for further analysis. The CEL isolations were performed in duplicate to quantitate the yields of CEL, and the yields were reported in average with standard deviation of the duplicates.

Gel permeation chromatographic (GPC) analysis

The weight-average molecular weight (M_w) and number-average molecular weight (M_n) of lignin were measured using GPC after acetylation as previously described⁵⁴. Briefly, The derivatization of lignin was conducted on a basis of ~3 mg lignin in 1 mL of 1:1 v/v pyridine/acetic anhydride in dark at room temperature for 24 h, 200 RPM. The solvent/reagents were removed by co-evaporation at 45°C with ethanol, several times, using a rotatory evaporator until dry. The resultant acetylated lignin was dissolved in tetrahydrofuran (THF) and the solution was filtered through 0.45 μ m membrane filter before GPC analysis. Size-exclusion separation was performed on an Agilent 1200 HPLC system (Agilent Technologies, Inc, Santa Clara, CA, US) equipped with Waters Styragel columns (HR1, HR2, and

HR6; Waters Corporation, Milford, MA, US). An UV detector (270 nm) was used for detection. THF was used as the mobile phase at a flowrate of 1.0 mL/min. Polystyrene narrow standards were used for establishing the calibration curve. The molar mass dispersity (D) was calculated as the ratio of M_w to M_n . The acetylation of lignin was conducted in duplicate. The results were report as an average with standard deviation.

NMR spectroscopic analysis

Nuclear magnetic resonance (NMR) spectra of isolated lignin samples were acquired in a Bruker Avance/DMX 400 MHz spectrometer and spectral processing used Bruker's Topspin 3.5 (Mac) software. A standard Bruker heteronuclear single quantum coherence (HSQC) pulse sequence (*hsqcetgp*) was used on a BBO probe with the following acquisition parameters: spectra width 10 ppm in F2 (^1H) dimension with 2,048 time of domain (acquisition time 256.1 ms), 210 ppm in F1 (^{13}C) dimension with 256 time of domain (acquisition time 6.1 ms), a 1.5-s delay, a 1J C–H of 145 Hz, and 32 scans. The central DMSO solvent peak ($\delta_{\text{C}}/\delta_{\text{H}}$ at 39.5/2.49) was used for chemical shifts calibration. Relative abundance of lignin compositional subunits and interunit linkage were estimated semi-quantitatively using volume integration of contours in HSQC spectra^{31, 49, 65}. For monolignol compositions of S, G, H, *p*-coumarate (*pCA*), and ferulate (FA) measurements, the $S_{2/6}$, G_2 , $H_{2/6}$, $pCA_{2/6}$, and FA_2 contours were used with G_2 and FA_2 integrals doubled. T_6 of triclin was used for contour integration. The C_{α} signals were used for contour integration for inter unit linkages estimation.

For quantitative ^{31}P NMR, CEL was phosphorylated with 2-chloro-4,4,5,5-tetramethyl-1,3,2-dioxaphospholane in a solvent of pyridine/ CDCl_3 (1.6/1.0 by v/v) according to published method.⁶⁶ In detail, 20.0 mg of CEL was accurately weighed into a 4-mL vial sealed with PTFE cap. A prepared stock solution of pyridine/deuterated chloroform (500 μL) including 1 mg/mL $\text{Cr}_{(\text{acac})_3}$ and 4 mg/mL internal standard (endo N-hydroxy-5-norbornene-2,3-dicarboxylic acid imide) was added to dissolve lignin. The phosphorylation was performed by adding 50 μL of the phosphorylating reagent TMDP (2-chloro-4,4,5,5-tetramethyl-1,3,2-dioxaphospholane). Quantitative ^{31}P NMR spectra were acquired on a Bruker Avance 400 MHz spectrometer equipped with a BBO probe using an inverse-gated decoupling pulse sequence (Waltz-16), 90° pulse, 25- μs pulse delay with 64 scans and a total runtime of 28 min. All chemical shifts reported are relative to the product of TMDP with water, which has been observed to give a sharp signal in pyridine/ CDCl_3 at 132.2 ppm. The contents of hydroxyl groups were quantitated on the basis of the amount of added internal standard. Quantitation of lignin hydroxyl groups were conducted in duplicate.

Thioacidolysis and triclin quantification

The triclin level in each lignin sample isolated from aerial roots, nodes, internodes, and seeds of Vanilla was quantified using the modified thioacidolysis method.⁶² Briefly, about 2.5 mg of dry plant material was accurately weighed into a 2-mL Micro-Reaction Vessel. One milliliter (1.0 mL) of thioacidolysis reagent was added to each vessel. The vials were capped tightly and put

into the position holes of a pre-heated MULTIVAP high-temperature dry block. The reaction was set at 100°C for 4 h with a brief vortex every hour. Upon completion of the reaction, the vials were placed in a rack at room temperature to cool. During the cooling time, 190 μL of saturated NaHCO_3 solution was added to 4-mL glass vials (Thermo Fisher Scientific, Waltham, USA, Cat. No. B7800-2), for LC–MS triclin analysis. Then, 400 μL of the cooled solution from the reaction vials was transferred into the 4-mL glass vials and mixed by pipetting. The 4-mL glass vials were placed in a dry block at 55°C under nitrogen gas flow until the samples had dried completely.

Triclin was quantified in biological duplicate by resuspending the dry sample in 600 μL of 95% methanol before subjecting to LC–MS. An Agilent HPLC 1290 infinity II system with Agilent 6460C Triple Quadrupole LC–MS System as mass detector was used. An Agilent Zorbax Eclipse Plus C18 column (2.1 mm \times 50 mm, 1.8- μm) was used to separate the compounds. The HPLC mobile phases used were 0.1% (v/v) formic acid in water (A) and 0.1% (v/v) formic acid in acetonitrile (B). The column thermostat was maintained at 30°C with a solvent flow rate of 0.45 mL/min, and the elution gradients were 6% B for 3 min, from 6 to 95% B in 5 min, stay in 95% B for 2 min, then from 95 to 6% B in 1 min and stay in 6% B for 2 min. The total run time was 13 min. Multiple reaction monitoring (MRM) mode for triclin quantification (the precursor and product ions for umbelliferone and triclin are m/z 161 and 133, and m/z 329 and 299, respectively). Nitrogen was used as sheath gas at a flow rate of 11 L/min at 350°C . The capillary gas temperature was 300°C , the flow rate 10 L/min, and the Nebulizer gas pressure 45 psi. The ESI spray capillary voltage was 3,500 V in negative ionization mode. The fragmentor voltage was 135 and the cell accelerator voltage was 7. Processing of data was done off-line using the Agilent Masshunter qualitative data analysis software.

Abbreviations

C2-Idf: CHALCONE SYNTHASE Colorless2 inhibitor diffuse
C3'H: *p*-coumaroyl ester 3-hydroxylase
CAD2: CINNAMYL ALCOHOL DEHYDROGENASE 2
CCoAOMT: caffeoyl coenzyme A 3-*O*-methyltransferase
COMT: caffeic acid-*O*-methyltransferase

Author Contributions

M.L.: conceptualization, methodology, investigation, data curation, writing-original draft. Y.P.: conceptualization, formal analysis, investigation, methodology, supervision, writing-review & editing. X.M.: investigation, data curation, writing-review & editing. F.C. and R.D.: resources and writing-review & editing. A.J.R.: conceptualization, methodology, supervision, writing-review & editing.

Conflicts of interest

There are no conflicts to declare.

Acknowledgements

This study was primarily supported and performed as part of the Center for Bioenergy Innovation (CBI), the USDA National Institute of Food and Agriculture, Hatch project 1012359, and The University of Tennessee Agricultural Experiment Station and AgResearch. CBI is a U.S. Department of Energy Bioenergy (DOE) Research Centers supported by the Office of Biological and Environmental Research in the DOE Office of Science. This work was partially funded by the Laboratory Directed Research and Development Program of Oak Ridge National Laboratory, managed by UT-Battelle, LLC, for the US Department of Energy under Contract DE-AC05-00OR22725. The United States Government retains and the publisher, by accepting the article for publication, acknowledges that the United States Government retains a nonexclusive, paid-up, irrevocable, worldwide license to publish or reproduce the published form of this manuscript, or allow others to do so, for United States Government purposes. The Department of Energy will provide public access to these results of federally sponsored research in accordance with the DOE Public Access Plan (<http://energy.gov/downloads/doe-public-access-plan>). The views and opinions of the authors expressed herein do not necessarily state or reflect those of the United States Government or any agency thereof. Neither the United States Government nor any agency thereof, nor any of their employees, makes any warranty, expressed or implied, or assumes any legal liability or responsibility for the accuracy, completeness, or usefulness of any information, apparatus, product, or process disclosed or represents that its use would not infringe privately owned rights.

References

- Ragauskas, A. J.; Beckham, G. T.; Biddy, M. J.; Chandra, R.; Chen, F.; Davis, M. F.; Davison, B. H.; Dixon, R. A.; Gilna, P.; Keller, M., Lignin valorization: improving lignin processing in the biorefinery. *Science* **2014**, *344* (6185), 1246843.
- Rinaldi, R.; Jastrzebski, R.; Clough, M. T.; Ralph, J.; Kennema, M.; Bruijninx, P. C.; Weckhuysen, B. M., Paving the way for lignin valorisation: recent advances in bioengineering, biorefining and catalysis. *Angew. Chem. Int. Ed.* **2016**, *55* (29), 8164-8215.
- Boerjan, W.; Ralph, J.; Baucher, M., Lignin biosynthesis. *Annu. Rev. Plant Biol.* **2003**, *54* (1), 519-546.
- del Río, J. C.; Rencoret, J.; Gutiérrez, A.; Elder, T.; Kim, H.; Ralph, J., Lignin monomers from beyond the canonical monolignol biosynthetic pathway: another brick in the wall. *ACS Sustainable Chemistry & Engineering* **2020**, *8* (13), 4997-5012.
- Cesarino, I.; Araújo, P.; Domingues Júnior, A. P.; Mazzafera, P., An overview of lignin metabolism and its effect on biomass recalcitrance. *Braz. J. Bot.* **2012**, *35* (4), 303-311.
- Li, M.; Pu, Y.; Ragauskas, A. J., Current understanding of the correlation of lignin structure with biomass recalcitrance. *Frontiers in Chemistry* **2016**, *4*.
- Ralph, J.; Lundquist, K.; Brunow, G.; Lu, F.; Kim, H.; Schatz, P. F.; Marita, J. M.; Hatfield, R. D.; Ralph, S. A.; Christensen, J. H., Lignins: natural polymers from oxidative coupling of 4-hydroxyphenyl-propanoids. *Phytochemistry reviews* **2004**, *3* (1), 29-60.
- Lam, P. Y.; Tobimatsu, Y.; Takeda, Y.; Suzuki, S.; Yamamura, M.; Umezawa, T.; Lo, C., Disrupting flavone synthase II alters lignin and improves biomass digestibility. *Plant Physiology* **2017**, *174* (2), 972-985.
- Lam, P. Y.; Lui, A. C.; Yamamura, M.; Wang, L.; Takeda, Y.; Suzuki, S.; Liu, H.; Zhu, F. Y.; Chen, M. X.; Zhang, J., Recruitment of specific flavonoid B-ring hydroxylases for two independent biosynthesis pathways of flavone-derived metabolites in grasses. *New Phytologist* **2019**, *223* (1), 204-219.
- Elder, T.; del Río, J. C.; Ralph, J.; Rencoret, J.; Kim, H.; Beckham, G. T.; Crowley, M. F., Coupling and reactions of lignols and new lignin monomers: A density functional theory study. *ACS Sustainable Chemistry & Engineering* **2020**, *8* (30), 11033-11045.
- Li, M.; Pu, Y.; Yoo, C. G.; Ragauskas, A. J., The occurrence of triclin and its derivatives in plants. *Green Chemistry* **2016**, *18* (6), 1439-1454.
- Zhou, J.-M.; Ibrahim, R. K., Tricin—a potential multifunctional nutraceutical. *Phytochem Rev.* **2010**, *9* (3), 413-424.
- Lan, W.; Rencoret, J.; Lu, F.; Karlen, S. D.; Smith, B. G.; Harris, P. J.; Del Río, J. C.; Ralph, J., Tricin-lignins: occurrence and quantitation of triclin in relation to phylogeny. *The Plant Journal* **2016**, *88* (6), 1046-1057.
- You, T.-T.; Mao, J.-Z.; Yuan, T.-Q.; Wen, J.-L.; Xu, F., Structural elucidation of the lignins from stems and foliage of *Arundo donax* Linn. *Journal of agricultural and food chemistry* **2013**, *61* (22), 5361-5370.
- Wen, J.-L.; Sun, S.-L.; Xue, B.-L.; Sun, R.-C., Quantitative structural characterization of the lignins from the stem and pith of bamboo (*Phyllostachys pubescens*). *Holzforchung* **2013**, *67* (6), 613-627.
- Rencoret, J.; Prinsen, P.; Gutiérrez, A.; Martínez, A. n. T.; del Río, J. C., Isolation and structural characterization of the milled wood lignin, dioxane lignin, and cellulolytic lignin preparations from brewer's spent grain. *Journal of agricultural and food chemistry* **2015**, *63* (2), 603-613.
- Mao, J.-Z.; Zhang, X.; Li, M.-F.; Xu, F., Effect of biological pretreatment with white-rot fungus *Trametes hirsuta* C7784 on lignin structure in *Carex meyeriana* Kunth. *BioResources* **2013**, *8* (3), 3869-3883.
- Rencoret, J.; Ralph, J.; Marques, G.; Gutiérrez, A.; Martínez, A. n. T.; del Río, J. C., Structural characterization of lignin isolated from coconut (*Cocos nucifera*) coir fibers. *Journal of agricultural and food chemistry* **2013**, *61* (10), 2434-2445.
- You, T.; Zhang, L.; Guo, S.; Shao, L.; Xu, F., Unraveling the Structural Modifications in Lignin of *Arundo donax* Linn. during Acid-Enhanced Ionic Liquid Pretreatment. *J. Agric. Food. Chem.* **2015**, *63* (50), 10747-10756.
- Liu, H.-M.; Li, H.-Y.; Li, M.-F., Cornstalk liquefaction in sub- and super-critical ethanol: Characterization of solid residue and the liquefaction mechanism. *Journal of the Energy Institute* **2017**, *90* (5), 734-742.
- Lan, W.; Lu, F.; Regner, M.; Zhu, Y.; Rencoret, J.; Ralph, S. A.; Zakai, U. I.; Morreel, K.; Boerjan, W.; Ralph, J., Tricin, a flavonoid monomer in monocot lignification. *Plant physiology* **2015**, *167* (4), 1284-1295.
- Fornalé, S.; Rencoret, J.; Garcia-Calvo, L.; Capellades, M.; Encina, A.; Santiago, R.; Rigau, J.; Gutiérrez, A.; Del Río, J.-C.; Caparros-Ruiz, D., Cell wall modifications triggered by the down-regulation of Coumarate 3-hydroxylase-1 in maize. *Plant Science* **2015**, *236*, 272-282.
- Singh, S. K.; Dhepe, P. L., Experimental evidences for existence of varying moieties and functional groups in assorted crop waste

- derived organosolv lignins. *Industrial Crops and Products* **2018**, *119*, 144-151.
24. Wu, M.; Pang, J.; Lu, F.; Zhang, X.; Che, L.; Xu, F.; Sun, R., Application of new expansion pretreatment method on agricultural waste. Part I: Influence of pretreatment on the properties of lignin. *Industrial Crops and Products* **2013**, *50*, 887-895.
25. Jiang, B.; Zhang, Y.; Gu, L.; Wu, W.; Zhao, H.; Jin, Y., Structural elucidation and antioxidant activity of lignin isolated from rice straw and alkali-oxygen black liquor. *International journal of biological macromolecules* **2018**, *116*, 513-519.
26. Takeda, Y.; Tobimatsu, Y.; Karlen, S. D.; Koshiha, T.; Suzuki, S.; Yamamura, M.; Murakami, S.; Mukai, M.; Hattori, T.; Osakabe, K., Downregulation of p-coumaroyl ester 3-hydroxylase in rice leads to altered cell wall structures and improves biomass saccharification. *The Plant Journal* **2018**, *95* (5), 796-811.
27. Koshiha, T.; Yamamoto, N.; Tobimatsu, Y.; Yamamura, M.; Suzuki, S.; Hattori, T.; Mukai, M.; Noda, S.; Shibata, D.; Sakamoto, M., MYB-mediated upregulation of lignin biosynthesis in *Oryza sativa* towards biomass refinery. *Plant Biotechnology* **2017**, *16*, 1201 a.
28. Del Río, J. C.; Rencoret, J.; Prinsen, P.; Martínez, A. n. T.; Ralph, J.; Gutiérrez, A., Structural characterization of wheat straw lignin as revealed by analytical pyrolysis, 2D-NMR, and reductive cleavage methods. *J. Agric. Food. Chem.* **2012**, *60* (23), 5922-5935.
29. Zikeli, F.; Ters, T.; Fackler, K.; Srebotnik, E.; Li, J., Successive and quantitative fractionation and extensive structural characterization of lignin from wheat straw. *Industrial Crops and Products* **2014**, *61*, 249-257.
30. Zeng, J.; Helms, G. L.; Gao, X.; Chen, S., Quantification of wheat straw lignin structure by comprehensive NMR analysis. *Journal of agricultural and food chemistry* **2013**, *61* (46), 10848-10857.
31. José, C.; Lino, A. G.; Colodette, J. L.; Lima, C. F.; Gutiérrez, A.; Martínez, Á. T.; Lu, F.; Ralph, J.; Rencoret, J., Differences in the chemical structure of the lignins from sugarcane bagasse and straw. *Biomass Bioenergy* **2015**, *81*, 322-338.
32. Mikhael, A.; Jurcic, K.; Fridgen, T. D.; Delmas, M.; Banoub, J., Matrix-assisted laser desorption/ionization time-of-flight/time-of-flight tandem mass spectrometry (negative ion mode) of French Oak lignin: A novel series of lignin and tricin derivatives attached to carbohydrate and shikimic acid moieties. *Rapid Communications in Mass Spectrometry* **2020**, *34* (18), e8841.
33. Miyamoto, T.; Takada, R.; Tobimatsu, Y.; Takeda, Y.; Suzuki, S.; Yamamura, M.; Osakabe, K.; Osakabe, Y.; Sakamoto, M.; Umezawa, T., Os MYB 108 loss-of-function enriches p-coumaroylated and tricin lignin units in rice cell walls. *The Plant Journal* **2019**, *98* (6), 975-987.
34. Eloy, N. B.; Voorend, W.; Lan, W.; Saleme, M. d. L. S.; Cesarino, I.; Vanholme, R.; Smith, R. A.; Goeminne, G.; Pallidis, A.; Morreel, K., Silencing CHALCONE SYNTHASE in maize impedes the incorporation of tricin into lignin and increases lignin content. *Plant Physiology* **2017**, *173* (2), 998-1016.
35. Liu, X.; Van Acker, R.; Voorend, W.; Pallidis, A.; Goeminne, G.; Pollier, J.; Morreel, K.; Kim, H.; Muylle, H.; Bosio, M., Rewired phenolic metabolism and improved saccharification efficiency of a *Zea mays* cinnamyl alcohol dehydrogenase 2 (*zmcad2*) mutant. *The Plant Journal* **2021**, *105* (5), 1240-1257.
36. Daly, P.; McClellan, C.; Maluk, M.; Oakey, H.; Lapiere, C.; Waugh, R.; Stephens, J.; Marshall, D.; Barakate, A.; Tsuji, Y., RNA i-suppression of barley caffeic acid O-methyltransferase modifies lignin despite redundancy in the gene family. *Plant biotechnology journal* **2019**, *17* (3), 594-607.
37. Eudes, A.; Dutta, T.; Deng, K.; Jacquet, N.; Sinha, A.; Benites, V. T.; Baidoo, E. E.; Richel, A.; Sattler, S. E.; Northen, T. R., SbCOMT (Bmr12) is involved in the biosynthesis of tricin-lignin in sorghum. *PLoS one* **2017**, *12* (6), e0178160.
38. Fornalé, S.; Rencoret, J.; García-Calvo, L.; Encina, A.; Rigau, J.; Gutiérrez, A.; Del Río, J. C.; Caparros-Ruiz, D., Changes in cell wall polymers and degradability in maize mutants lacking 3'- and 5'-O-methyltransferases involved in lignin biosynthesis. *Plant and Cell Physiology* **2017**, *58* (2), 240-255.
39. Lam, P. Y.; Tobimatsu, Y.; Matsumoto, N.; Suzuki, S.; Lan, W.; Takeda, Y.; Yamamura, M.; Sakamoto, M.; Ralph, J.; Lo, C., OsCALD1 is a bifunctional O-methyltransferase involved in the biosynthesis of tricin-lignins in rice cell walls. *Scientific reports* **2019**, *9* (1), 1-13.
40. Lan, W.; Morreel, K.; Lu, F.; Rencoret, J.; del Río, J. C.; Voorend, W.; Vermerris, W.; Boerjan, W. A.; Ralph, J., Maize Tricin-Oligolignol Metabolites and Their Implications for Monocot Lignification. *Plant physiology* **2016**, pp. 02012.2016.
41. Lauberte, L.; Telysheva, G.; Cravotto, G.; Andersone, A.; Janceva, S.; Dizhbite, T.; Arshanitsa, A.; Jurkane, V.; Veveř, L.; Grillo, G., Lignin-Derived antioxidants as value-added products obtained under cavitation treatments of the wheat straw processing for sugar production. *Journal of Cleaner Production* **2021**, *303*, 126369.
42. Chang, H.-m.; Cowling, E. B.; Brown, W., Comparative studies on cellulolytic enzyme lignin and milled wood lignin of sweetgum and spruce. *Holzforchung-International Journal of the Biology, Chemistry, Physics and Technology of Wood* **1975**, *29* (5), 153-159.
43. Guerra, A.; Filpponen, I.; Lucia, L. A.; Saquing, C.; Baumberger, S.; Argyropoulos, D. S., Toward a better understanding of the lignin isolation process from wood. *J. Agric. Food. Chem.* **2006**, *54* (16), 5939-5947.
44. Chen, F.; Tobimatsu, Y.; Havkin-Frenkel, D.; Dixon, R. A.; Ralph, J., A polymer of caffeyl alcohol in plant seeds. *Proceedings of the National Academy of Sciences* **2012**, *109* (5), 1772-1777.
45. Ghaffar, S. H.; Fan, M.; Zhou, Y.; Abo Madyan, O., Detailed analysis of wheat straw node and internode for their prospective efficient utilization. *Journal of agricultural and food chemistry* **2017**, *65* (41), 9069-9077.
46. Wen, J.-L.; Sun, S.-L.; Xue, B.-L.; Sun, R.-C., Recent advances in characterization of lignin polymer by solution-state nuclear magnetic resonance (NMR) methodology. *Materials* **2013**, *6* (1), 359-391.
47. Tobimatsu, Y.; Chen, F.; Nakashima, J.; Escamilla-Treviño, L. L.; Jackson, L.; Dixon, R. A.; Ralph, J., Coexistence but independent biosynthesis of catechyl and guaiacyl/syringyl lignin polymers in seed coats. *The Plant Cell* **2013**, *25* (7), 2587-2600.
48. Su, S.; Wang, S.; Song, G., Disassembling catechyl and guaiacyl/syringyl lignins coexisting in Euphorbiaceae seed coats. *Green Chemistry* **2021**.
49. Mansfield, S. D.; Kim, H.; Lu, F.; Ralph, J., Whole plant cell wall characterization using solution-state 2D NMR. *Nature protocols* **2012**, *7* (9), 1579-1589.
50. Yoo, C. G.; Pu, Y.; Li, M.; Ragauskas, A. J., Elucidating Structural Characteristics of Biomass using Solution-State 2 D NMR with a Mixture of Deuterated Dimethylsulfoxide and Hexamethylphosphoramide. *ChemSusChem* **2016**, *9* (10), 1090-1095.
51. Pu, Y.; Cao, S.; Ragauskas, A. J., Application of quantitative 31P NMR in biomass lignin and biofuel precursors characterization. *Energy & Environmental Science* **2011**, *4* (9), 3154-3166.
52. Li, M.; Pu, Y.; Tschaplinski, T. J.; Ragauskas, A. J., 31P NMR Characterization of Tricin and Its Structurally Similar Flavonoids. *ChemistrySelect* **2017**, *2* (12), 3557-3561.
53. Heikkinen, H.; Elder, T.; Maaheimo, H.; Rovio, S.; Rahikainen, J.; Kruus, K.; Tamminen, T., Impact of steam explosion on the wheat

straw lignin structure studied by solution-state nuclear magnetic resonance and density functional methods. *J. Agric. Food. Chem.* **2014**, *62* (43), 10437-10444.

54. Samuel, R.; Pu, Y.; Jiang, N.; Fu, C.; Wang, Z.-Y.; Ragauskas, A., Structural characterization of lignin in wild-type versus COMT down-regulated switchgrass. *Front Energy Res* **2014**, *1*, 1-9.

55. Jiang, B.; Song, J.; Jin, Y., A flavonoid monomer triclin in gramineous plants: metabolism, bio/chemosynthesis, biological properties, and toxicology. *Food chemistry* **2020**, *320*, 126617.

56. Lam, P. Y.; Lui, A. C.; Wang, L.; Liu, H.; Umezawa, T.; Tobimatsu, Y.; Lo, C., Tricin Biosynthesis and Bioengineering. *Frontiers in Plant Science* **2021**, *12*.

57. van Erven, G.; Nayan, N.; Sonnenberg, A. S.; Hendriks, W. H.; Cone, J. W.; Kabel, M. A., Mechanistic insight in the selective delignification of wheat straw by three white-rot fungal species through quantitative ¹³C-1S py-GC-MS and whole cell wall HSQC NMR. *Biotechnology for biofuels* **2018**, *11* (1), 1-16.

58. Tarmadi, D.; Tobimatsu, Y.; Yamamura, M.; Miyamoto, T.; Miyagawa, Y.; Umezawa, T.; Yoshimura, T., NMR studies on lignocellulose deconstructions in the digestive system of the lower termite *Coptotermes formosanus* Shiraki. *Scientific reports* **2018**, *8* (1), 1290.

59. Lapiere, C.; Monties, B.; Rolando, C.; Chirale, L. d., Thioacidolysis of lignin: comparison with acidolysis. *J. Wood Chem. Technol.* **1985**, *5* (2), 277-292.

60. Lapiere, C.; Pollet, B.; Rolando, C., New insights into the molecular architecture of hardwood lignins by chemical degradative methods. *Res. Chem. Intermed.* **1995**, *21* (3), 397-412.

61. Holtman, K. M.; Chang, H.-M.; Jameel, H.; Kadla, J. F., Elucidation of lignin structure through degradative methods: Comparison of modified DFRC and thioacidolysis. *J. Agric. Food. Chem.* **2003**, *51* (12), 3535-3540.

62. Chen, F.; Zhuo, C.; Xiao, X.; Pendergast, T. H.; Devos, K. M., A rapid thioacidolysis method for biomass lignin composition and triclin analysis. *Biotechnology for biofuels* **2021**, *14* (1), 1-9.

63. Jiang, B.; Cao, T.; Gu, F.; Wu, W.; Jin, Y., Comparison of the structural characteristics of cellulolytic enzyme lignin preparations isolated from wheat straw stem and leaf. *ACS Sustainable Chemistry & Engineering* **2017**, *5* (1), 342-349.

64. Hu, Z.; Yeh, T.-F.; Chang, H.-m.; Matsumoto, Y.; Kadla, J. F., Elucidation of the structure of cellulolytic enzyme lignin. *Holzforchung* **2006**, *60* (4), 389-397.

65. Kim, H.; Ralph, J., A gel-state 2D-NMR method for plant cell wall profiling and analysis: a model study with the amorphous cellulose and xylan from ball-milled cotton linters. *Rsc Advances* **2014**, *4* (15), 7549-7560.

66. Meng, X.; Crestini, C.; Ben, H.; Hao, N.; Pu, Y.; Ragauskas, A. J.; Argyropoulos, D. S., Determination of hydroxyl groups in biorefinery resources via quantitative ³¹P NMR spectroscopy. *Nature Protocols* **2019**, *14* (9), 2627-2647.